

PHASE VARIATION IN THE PULSE PROFILE OF SMC X-1

J. NEILSEN^{1,2}, R.C. HICKOX², AND S.D. VRTILEK²
Accepted for publication in Astrophysical Journal Letters

ABSTRACT

We present the results of the timing and spectral analysis of X-ray high-state observations of the high-mass X-ray pulsar SMC X-1 with *Chandra*, *XMM-Newton*, and *ROSAT*, taken between 1991 and 2001. The source has $L_X \sim (3-5) \times 10^{38}$ ergs s⁻¹, and the spectra can be modeled as a power law plus blackbody with $kT_{\text{BB}} \sim 0.18$ keV and a reprocessed emission radius $R_{\text{BB}} \sim 2 \times 10^8$ cm, assuming a distance of 60 kpc to the source. Energy-resolved pulse profiles show several distinct forms, more than half of which include a second pulse in the soft profile, previously documented only in hard energies. We also detect significant variation in the phase shift between hard and soft pulses, as has recently been reported in Her X-1. We suggest an explanation for the observed characteristics of the soft pulses in terms of precession of the accretion disk.

Subject headings: accretion, accretion disks — stars: neutron — X-rays: binaries: individual (SMC X-1) — stars: pulsars: individual (SMC X-1)

1. INTRODUCTION

SMC X-1 is a high-mass X-ray binary system consisting of an X-ray source, a $1.6 M_{\odot}$ pulsar, accreting from a $17.2 M_{\odot}$ companion, Sk 160 (Clarkson et al. 2003). It is also the only X-ray pulsar for which no spin-down episodes have been observed (Kahabka & Li 1999). The X-ray pulsar has a spin period of 0.71 s and an eclipsing orbital period of 3.89 days, and in addition it shows a superorbital variation in flux with period between 45 and 60 days. This is likely due to precession of a warped accretion disk (Wojdowski et al. 1998).

The presence of the accretion disk is likely to have significant consequences for the observed pulse profile. In Her X-1, a low-mass X-ray pulsar with a regular 35 day superorbital period, reprocessing of hard X-rays by the disk gives rise to a pulsating, soft spectral component (Endo et al. 2000). Zane et al. (2004) have shown that the phase difference between hard and soft pulses changes as the accretion disk precesses. If similar reprocessing is at work in SMC X-1, as argued by Hickox et al. (2004), the pulse profiles should show a variation similar to that of Her X-1. To that end, we have analyzed pulse profiles of SMC X-1 in different epochs from *Chandra*, *XMM*, and *ROSAT*. In § 2 we discuss the observations and our methods of data analysis. In § 3 we present the results of our analysis, and in § 4 we consider the implications of our results and future work.

2. OBSERVATIONS

The observations reported in this Letter are described in Table 1 and were made with *Chandra*'s ACIS-S in continuous clocking (CC) mode (CXC Proposers' Observatory Guide v5.0, 2002), the EPIC-pn detectors on *XMM-Newton* in full window (X101) and small window (X201) modes (XMM-Newton Users' Handbook v2.2, 2004), and the *ROSAT* PSPC detectors in pointing mode (ROSAT Users' Handbook 1996). We shall refer to the observations as C104, X201, Rn00, etc. (see Table 1). Fig. 1 locates the *Chandra* and *XMM* observations in the All-Sky Monitor (ASM) lightcurve from the *Ross* X-ray Timing Explorer (*RXTE*) mission. We estimate the su-

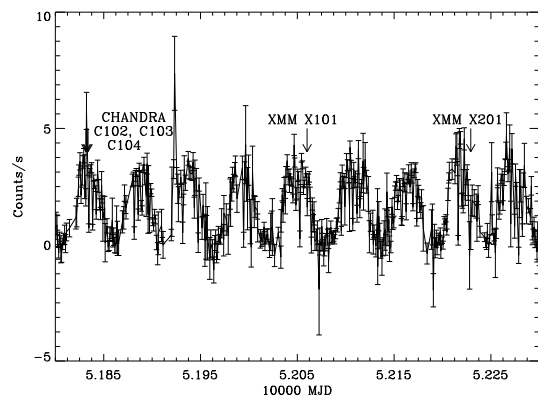


FIG. 1.— *RXTE* ASM lightcurve for SMC X-1 with arrows designating several observations. Quick-look results as provided by the *RXTE*/ASM team.

perorbital phase (ϕ_{SO}) as 0.16 for the *Chandra* observations, 0.37 for X101, and 0.42 for X201, where $\phi_{\text{SO}} = 0$ at the beginning of the X-ray high state. Given the variation in ϕ_{SO} , the uncertainty for these estimates is plus or minus a few days or $\phi_{\text{SO}} \sim 0.05$. The ϕ_{SO} estimates for *ROSAT* are unavailable because those observations were taken before the launch of *RXTE*.

Since the CC mode provides only one dimension of spatial information, ACIS source events were extracted from a source-centered rectangle of size $0''.492 \times 1''.968$. Background events were extracted from two regions $0''.492 \times 9''.84$ equidistant from the source. For X101, which shows the source entering an eclipse, events were located within a circular region of radius $45''$ and extracted from the 4.9 ks of pre-eclipse data; for X201, we used a circular region of radius $51''.2$. We ignored the *XMM* background because its surface brightness was less than 0.1% of that of the source region. *ROSAT* source events were extracted from a circular region of radius $2''.5$. For Ra02, which shows an eclipse, events were taken from the 5.5 ks of post-eclipse data.

3. ANALYSIS

Before the spectroscopic and timing analysis, we performed a barycentric correction and corrected for the orbital motion of SMC X-1 using the orbital ephemeris calculated by

¹ Kenyon College, Department of Physics, Gambier, OH 43022; neilsenj@kenyon.edu

² Harvard-Smithsonian Center for Astrophysics, 60 Garden Street, Cambridge, MA 02138; rhickox@cfa.harvard.edu; saku@head.cfa.harvard.edu

TABLE 1
OBSERVATIONS OF SMC X-1

Observation ID Number	Observation Reference	Mission	Start Time (JD-2400000)	Observation Time (ks)	Period (s)
rp400022n00	Rn00	<i>ROSAT</i>	48536.67	16.6	0.709114(2)
rp400022a02	Ra02	<i>ROSAT</i>	49141.50	11.8	0.708598(5)
400102	C102	<i>Chandra</i>	51832.17	6.2	0.70567(2)
400103	C103	<i>Chandra</i>	51833.34	6.1	0.70567(2)
400104	C104	<i>Chandra</i>	51834.31	6.5	0.70567(1)
0011450101	X101	<i>XMM</i>	52060.59	46.4	0.70542(2)
0011450201	X201	<i>XMM</i>	52229.65	40.0	0.70522(3)

Wojdowski et al. (1998). The following analysis was performed with CIAO version 3.1 for *Chandra* and *ROSAT* data and SAS version 5.3.3 for *XMM*.

3.1. Phase-Averaged Spectroscopy

For *Chandra* and *XMM*, we extracted phase-averaged spectra, modeling the 0.6–9.8 keV emissions with neutral absorption, a blackbody with $kT_{\text{BB}} \sim 0.18$ keV, and a power law. For the *XMM* spectra we also included a high-energy cutoff ($E_{\text{cut}} \sim 6$ keV, $E_{\text{fold}} \sim 8$ keV Woo et al. 1995). For *Chandra* and X201, we excluded the energy range 1.7–2.8 keV to avoid instrumental effects (near the Au and Si edges) for high count data (Miller et al. 2002). Although the excellent time resolution of CC mode prevents some photon pileup, we used the ISIS pileup kernel for the *Chandra* observations (Davis 2001), which show a pileup fraction of $\sim 17\%$. For *XMM* we minimized pileup in the spectra by excluding events from the central one-third radius of the extraction regions.

Spectral fits from C104, X201, and X101 are shown in Fig. 2 and results are listed in Table 2. All spectra are dominated by blackbody emission below ~ 1.0 keV, although the similar wavy residuals in the *Chandra* and X201 spectra below 1.0 keV suggest that the soft emission is not exactly blackbody. For X101, the data are taken as the source is entering eclipse, and the spectrum could not be fitted using the simple model above. Fixing Γ to a typical value of 0.9, we found that a good fit is achieved by including a partial covering absorption, with a covering fraction of 88%. This accounts for the extra absorption by the dense gas around the star as the eclipse begins, but allows for some X-rays to be scattered around the absorbing region. Residuals suggest that there may also be Fe absorption at ~ 6.5 keV, but more detailed spectral analysis is beyond the scope of this Letter. Since blackbody emission dominates below 1.0 keV, and power-law emission above 2.0 keV, we can use energy-resolved profiles in these ranges to examine the variation of the separate components. More detailed analysis, using pulse-phase spectroscopy, will be presented in a forthcoming paper.

3.2. Timing Analysis

Since SMC X-1 is a fast-period pulsar, pulse profile analysis requires a time resolution of better than 0.71 s. Fortunately, the *Chandra*, X201, X101, and *ROSAT* observations have sufficient time resolutions of 2.85, 6, 73.4, and 130 ms, respectively. We used *efsearch* in the software package XRONOS to measure the pulse periods (see Table 1). These are consistent with the spin-up rate calculated by Wojdowski et al. (1998) and the periods determined by Vrtilik et al. (2001) from the same *Chandra* data. We extracted high- and low-energy pulse profiles from each of the seven observations (see Fig. 3). Here

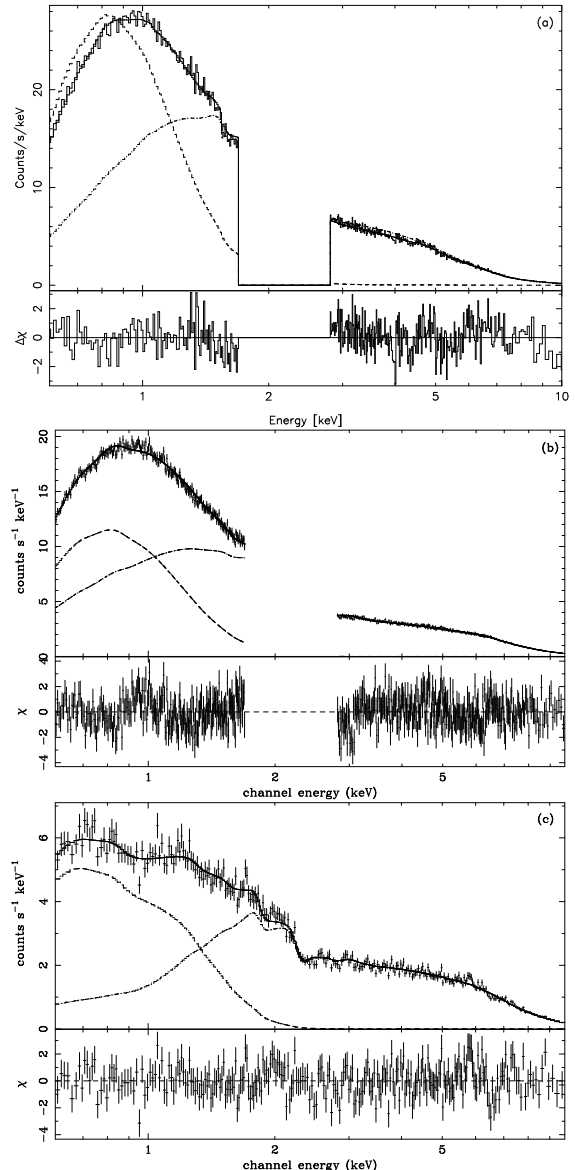
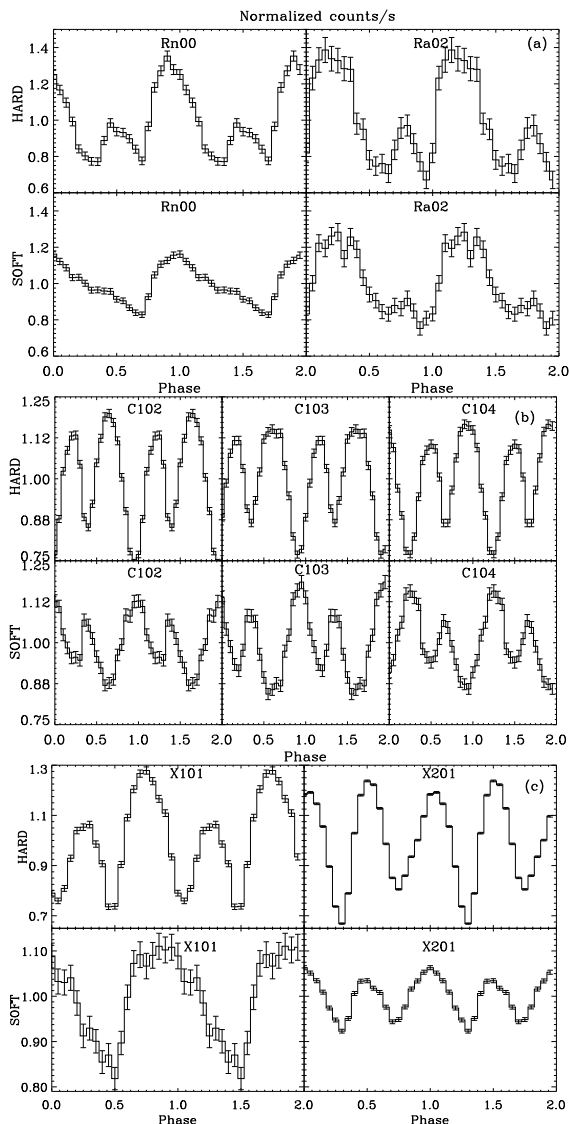


FIG. 2.— Spectra from (a) C104, (b) X201, and (c) X101 with blackbody and power law components shown. As X101 is a pre-eclipse observation, it was fit with an additional partial covering absorption. Note that in (a) the model components do not add exactly to the observed counts. This is due to the pileup kernel used in the fit.

TABLE 2
 FITS TO SMC X-1 SPECTRA

Parameter	C102	C103	C104	X201	X101
N_H	$0.14^{+0.02}_{-0.02}$	$0.23^{+0.02}_{-0.02}$	$0.19^{+0.01}_{-0.01}$	$0.17^{+0.01}_{-0.01}$	$0.08^{+0.02}_{-0.02}$
Γ	$0.89^{+0.03}_{-0.04}$	$1.03^{+0.03}_{-0.04}$	$0.92^{+0.03}_{-0.04}$	$0.91^{+0.02}_{-0.02}$	0.9
kT_{BB}	$0.177^{+0.007}_{-0.007}$	$0.169^{+0.005}_{-0.005}$	$0.178^{+0.005}_{-0.005}$	$0.190^{+0.004}_{-0.004}$	$0.173^{+0.013}_{-0.010}$
E_{cut} (keV)	$6.1^{+0.1}_{-0.1}$	$5.9^{+0.2}_{-0.2}$
E_{fold} (keV)	$6.8^{+0.3}_{-0.3}$	$8.9^{+1.1}_{-1.2}$
Pileup fraction	0.16	0.18	0.16
Partial N_H (10^{22}cm^{-2})	$1.2^{+0.1}_{-0.1}$
Covering fraction	$0.88^{+0.02}_{-0.03}$
χ^2 (d.o.f.)	1.36 (384)	1.19 (387)	1.22 (390)	1.20 (516)	1.20 (258)
Observed flux ($10^{-9} \text{ergs cm}^{-2} \text{s}^{-1}$)	1.1	1.1	1.1	1.0	0.57
Unabsorbed flux ($10^{-9} \text{ergs cm}^{-2} \text{s}^{-1}$)	1.2	1.2	1.3	1.1	0.84
Luminosity (ergs s^{-1})	5.2	5.3	5.4	4.7	3.6

NOTE. — Errors are 90% confidence for a single parameter. Fluxes are for 0.6–9.8 keV. A distance of 60 kpc is assumed for the SMC.


 FIG. 3.— Hard and soft pulse profiles for (a) *ROSAT*, (b) *Chandra*, and (c) *XMM*. The hard range is 2.0–8.0 keV (1.5–2.4 keV for *ROSAT*); soft is 0.5–1.0 keV. Two pulse periods are shown for clarity. Note that the pulse phases shown are not absolute, but are only relative to each observation.

we do not correct for pileup effects, since these have minimal impact on the shapes of the pulses.

All seven observations show the double-peaked hard pulse profile that has been thoroughly documented (Wojdowski et al. 1998; Paul et al. 2002; Naik & Paul 2004). The soft profile, however, varies markedly. While earlier studies of SMC X-1 have shown a roughly sinusoidal shape of soft pulses (Paul et al. 2002; Naik & Paul 2004), the *ROSAT*, *Chandra*, and *XMM* observations show a complex variation of profiles. Although the *ROSAT* pulse profiles show a single main soft peak, four of the five *Chandra* and *XMM* observations show *double*-peaked soft pulses.

The first *ROSAT* observation, Rn00, shows a single asymmetric hump at lower energies, slightly out of phase with the hard pulses. For Ra02, the soft pulses are lightly double-peaked, although the poor spectral resolution of the PSPC places the exact details of the profiles in doubt. The X101 pulse profile shows a single broad peak quite similar to Rn00. In the *Chandra* data, we see a clear second peak in all three soft pulse profiles, and we note a *significant phase difference* between hard and soft pulses. In X201 we also find double-peaked soft pulses, but these are *almost in phase* with the hard pulses.

For *Chandra* and *XMM* we cross-correlated the hard and soft profiles, to quantify the phase shift between the pulses (see Fig. 4), as in Ramsay et al. (2002) and Zane et al. (2004). The *Chandra* profiles show strong anticorrelations at a phase shift of 0° and positive correlations at $\pm 90^\circ$. We see multiple peaks because the hard and soft profiles each have two pulses. Observation X101 shows a broad correlation with a peak at $\sim 20^\circ$; in X201 we detect possible phase shifts of $\sim 0^\circ$, $\sim \pm 90^\circ$, and $\sim \pm 170^\circ$.

4. DISCUSSION

In these observations both hard and soft X-rays show pulsations, but differences in the hard and soft pulse profiles indicate a different geometric or physical origin of emission (Paul et al. 2002). Soft pulses in the most luminous X-ray pulsars are likely to originate at the inner edge of the accretion disk, where hard pulses from the neutron star are reradiated at lower energies by disk gases (Hickox et al. 2004). If this picture is valid for SMC X-1, the observed blackbody component should be consistent with emission from the inner disk. For reprocessing by a partial spherical surface around the neutron

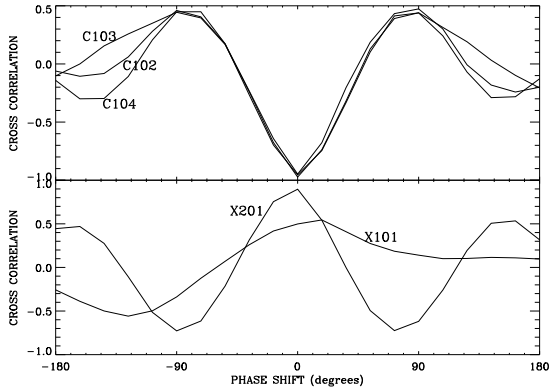


FIG. 4.— Cross-correlation between hard and soft pulse profiles for *Chandra* and *XMM* data.

star, the blackbody radius R_{BB} is given by (Paul et al. 2002)

$$R_{\text{BB}} = \sqrt{\frac{L_X}{4\pi\sigma T_{\text{BB}}^4}}.$$

Using $kT_{\text{BB}} \sim 0.18$ keV and $L_X \sim 4 \times 10^{38}$ ergs s^{-1} , we have $R_{\text{BB}} \sim 1.7 \times 10^8$ cm.

In the standard model for X-ray pulsars, the inner disk radius R_0 is close to the magnetospheric radius R_m , where the magnetic pressure of the dipole field equals the ram pressure of the infalling gas. However, R_m is difficult to estimate for SMC X-1, because the surface B -field has not been directly measured. We note that R_{BB} is close to the corotation radius $R_{\text{cor}} = (GMP^2/4\pi^2)^{1/3} \simeq 1.3 \times 10^8$ cm, which is another estimate for R_0 . However, the lack of spin-down episodes for SMC X-1 suggests that $R_0 < R_{\text{cor}}$ (Kahabka & Li 1999). The situation is therefore unclear, but without additional constraints it is certainly possible that the soft pulses originate at the inner accretion disk.

In light of this picture we consider the following pulse profile characteristics:

1. The hard pulse profile is consistently double-peaked, typically with one dominant peak.
2. The soft pulse profile varies in shape, and has been observed with either a single asymmetric peak or two peaks with varying degrees of symmetry.

3. The pulse profiles exhibit large-scale variations in phase relationship. Closely-spaced observations have revealed identical phase shifts.

Zane et al. (2004) suggest that the varying hard-soft phase shift in Her X-1 may be due to the precession of the accretion disk, so we consider the possibility that such a disk could reproduce the above characteristics in SMC X-1. If the observational line of sight is sufficiently close to the plane of the magnetic axis, we might always see two hard pulses, one from each magnetic pole. However, the soft profile could change dramatically in shape and relative phase, as observed, if precession of the disk causes the visible part of the reprocessing region to vary.

We note however that we cannot conclusively verify this picture and its analogy to Her X-1. First, we lack sufficient sampling of the full 60 day superorbital period. Second, the hard-soft phase shift appears to vary more rapidly for SMC X-1 (a change of $\simeq 90^\circ$ between $\phi_{\text{SO}} \simeq 0.16$ and 0.42) than for Her X-1 ($\simeq 20^\circ$ between $\phi_{\text{SO}} \simeq 0.03$ and 0.17 Zane et al. 2004). Third, it is not completely clear even in Her X-1 that the phase variation is caused by the 35 day disk precession; soon after the observations of Zane et al. (2004), the source entered an anomalous low state, an event that may be caused by changes in the inner disk structure (Boyd & Still 2004; Oosterbroek et al. 2001). Such changes could alter the shape of the inner reprocessing region, and thus the soft profiles, in a way that is not directly related to the superorbital period.

We conclude that in SMC X-1, we have observed variations in the soft pulse profile that likely reflect changes in the reprocessing of hard X-rays by the accreting gas. These variations may be related to the superorbital precession of the accretion disk, as has been proposed for Her X-1. If it can be shown with more observations that the pulse profiles and superorbital period are correlated, then we will have the opportunity to apply significant constraints to the geometry of SMC X-1.

We thank Cara Rakowski, John Houck, Craig Heinke, Jonathan McDowell, and Patrick Wojdowski for helpful discussions and the referee for useful comments. This work was supported in part by NSF grants 9731923 and AST 0307433 and NASA grant NAG5-10780.

REFERENCES

- Boyd, P. & Still, M. 2004, *The Astronomer's Telegram*, 228, 1
 Clarkson, W. I., Charles, P. A., Coe, M. J., Laycock, S., Tout, M. D., & Wilson, C. A. 2003, *MNRAS*, 339, 447
 Davis, J. E. 2001, *ApJ*, 562, 575
 Endo, T., Nagase, F., & Mihara, T. 2000, *PASJ*, 52, 223
 Hickox, R. C., Narayan, R., & Kallman, T. R. 2004, *ApJ*, in press (v614, Oct 2004, astro-ph/0407115)
 Kahabka, P. & Li, X.-D. 1999, *A&A*, 345, 117
 Miller, J. M., Fabian, A. C., Wijnands, R., Remillard, R. A., Wojdowski, P., Schulz, N. S., Di Matteo, T., Marshall, H. L., Canizares, C. R., Pooley, D., & Lewin, W. H. G. 2002, *ApJ*, 578, 348
 Naik, S. & Paul, B. 2004, *A&A*, 418, 655
 Oosterbroek, T., Parmar, A. N., Orlandini, M., Segreto, A., Santangelo, A., & Del Sordo, S. 2001, *A&A*, 375, 922
 Paul, B., Nagase, F., Endo, T., Dotani, T., Yokogawa, J., & Nishiuchi, M. 2002, *ApJ*, 579, 411
 Ramsay, G., Zane, S., Jimenez-Garate, M. A., den Herder, J., & Hailey, C. J. 2002, *MNRAS*, 337, 1185
 Vrtillek, S. D., Raymond, J. C., Boroson, B., Kallman, T., Quintrell, H., & McCray, R. 2001, *ApJ*, 563, L139
 Wojdowski, P., Clark, G. W., Levine, A. M., Woo, J. W., & Zhang, S. N. 1998, *ApJ*, 502, 253
 Woo, J. W., Clark, G. W., Blondin, J. M., Kallman, T. R., & Nagase, F. 1995, *ApJ*, 445, 896
 Zane, S., Ramsay, G., Jimenez-Garate, M. A., Willem den Herder, J., & Hailey, C. J. 2004, *MNRAS*, 350, 506